

Received 27 February 2020
Accepted 30 March 2020

Edited by W. T. A. Harrison, University of Aberdeen, Scotland

Keywords: oxychloride; rare-earth oxyhalide; powder diffraction.

CCDC reference: 1993793

Supporting information: this article has supporting information at journals.iucr.org/e

Dehydration synthesis and crystal structure of terbium oxychloride, TbOCl

Saehma Chong,* Brian J. Riley and Zayne J. Nelson

Pacific Northwest National Laboratory, Richland, WA 99352, USA. *Correspondence e-mail: saehwa.chong@pnnl.gov

Terbium oxychloride, TbOCl, was synthesized *via* the simple heat-treatment of $\text{TbCl}_3 \cdot 6\text{H}_2\text{O}$ and its structure was determined by refinement against X-ray powder diffraction data. TbOCl crystallizes with the matlockite (PbFCl) structure in the tetragonal space group $P4/nmm$ and is composed of alternating (001) layers of $(\text{TbO})_n$ and $n \text{Cl}^-$. The unit-cell parameters, unit-cell volume, and density were compared to the literature data of other isostructural rare-earth oxychlorides in the same space group and showed good agreement when compared to the calculated trendlines.

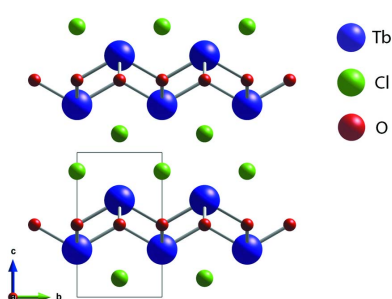
1. Chemical context

Rare-earth oxychlorides, $RE\text{OCl}$, are promising materials for various applications including use as catalysts, sensors, and phosphors (Podkolzin *et al.*, 2007; Au *et al.*, 1997; Peringer *et al.*, 2009; Marsal *et al.*, 2005; Kim *et al.*, 2019; Berdowski *et al.*, 1984; Imanaka *et al.*, 2001a,b; Okamoto *et al.*, 2002; Kim *et al.*, 2014). LaOCl is a stable catalyst for converting methane to methyl chloride (Podkolzin *et al.*, 2007) and can be used as a sensor material to detect CO_2 and Cl_2 gases (Marsal *et al.*, 2005; Imanaka *et al.*, 2001b). The EuOCl catalyst showed high efficiency in converting ethylene to vinyl chloride (Scharfe *et al.*, 2016). The luminescent properties of $REOX$ ($RE = \text{La}, \text{Eu}; X = \text{F}, \text{Cl}, \text{Br}, \text{I}$) can be controlled to emit a wide range of visible light from blue to red by changing the crystal symmetries and compositions (Kim *et al.*, 2014, 2019). As part of our studies in this area, we now describe the dehydration synthesis and structure of the title compound.

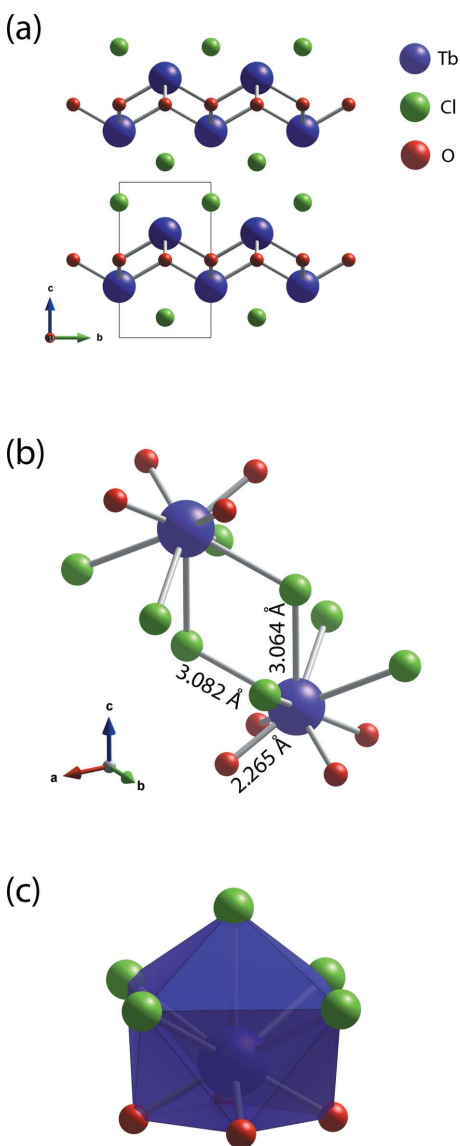
2. Structural commentary

The structural parameters of $RE\text{OCl}$ ($RE = \text{La}, \text{Ce}, \text{Pr}, \text{Nd}, \text{Sm}, \text{Eu}, \text{Gd}, \text{Tb}, \text{Dy}, \text{Ho}$) in the literature and current study are summarized in Table 1. All these $RE\text{OCl}$ compounds crystallize in the matlockite (PbFCl ; Bannister, 1934) structure within the tetragonal $P4/nmm$ space group. The crystal structure of TbOCl contains alternating (001) layers of $(\text{TbO})_n$ and $n \text{Cl}^-$ (Fig. 1a). The Tb cation is coordinated by five chloride ions and four oxygen atoms, forming a mono-capped TbO_4Cl_5 square antiprism (Fig. 1b and 1c). The $RE-\text{Cl}$ and $RE-\text{O}$ bond lengths in the $RE\text{OCl}$ compounds are provided in Table 1. With larger RE cations in the structures, the $RE-\text{Cl}$ and $RE-\text{O}$ bond lengths increase (Fig. 2).

The shortest $\text{Cl}\cdots\text{Cl}$ separation in TbOCl is 3.271 (4) Å, which compares with the van der Waals diameter of a Cl^- ion of about 3.62 Å. The $\text{Cl}\cdots\text{Cl}$ distances of other $RE\text{OCl}$ compounds are also short, ranging from 3.24 to 3.46 Å on



OPEN ACCESS

**Figure 1**

(a) Crystal structure of TbOCl, (b) the coordination environment of Tb, and (c) polyhedron representation of the Tb environment.

going from Ho³⁺ to La³⁺. With non-bonded vectors shorter than the van der Waals separation, strong interactions between atoms are expected in the structure (Maslen *et al.*, 1996). Templeton & Dauben (1953) mention the presence of weaker anion–anion repulsion between Cl atoms in REOCl structures. The structural parameters of TbOCl were compared with the trendlines calculated using the values from Table 1 (Fig. 3). The unit-cell parameters and volumes increase linearly with the larger RE cations (Shannon, 1976) whereas the densities decrease non-linearly, fitting well to a 2nd order polynomial trend.

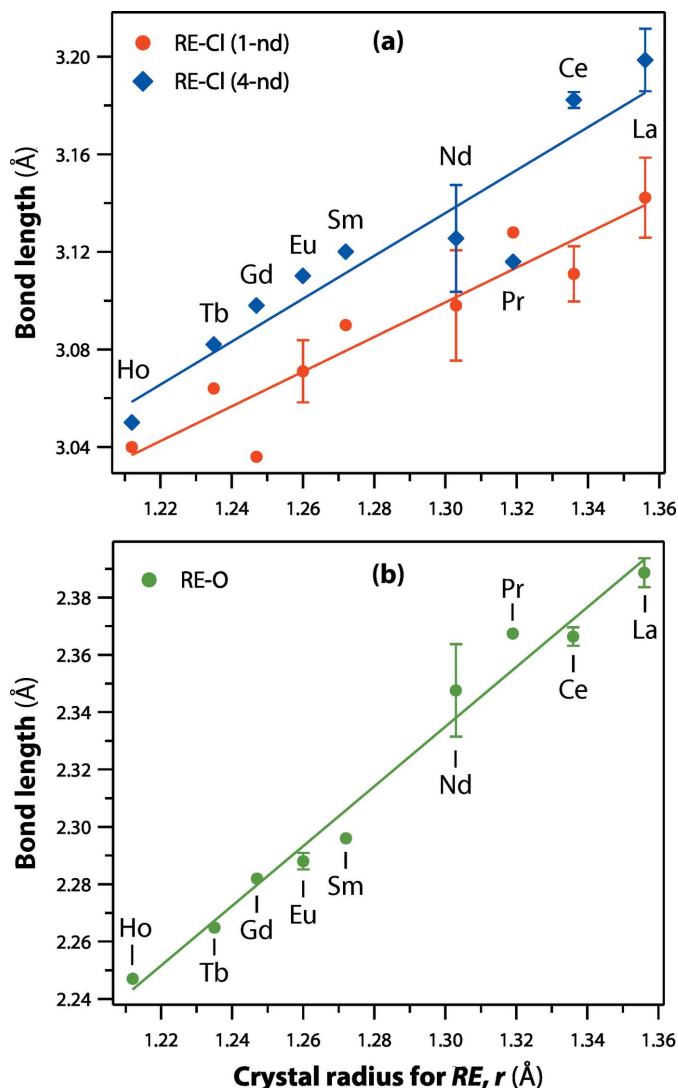
3. Synthesis and crystallization

The title compound was synthesized by a simple heat treatment of TbCl₃·6H₂O (Alfa Aesar, 99.99%). About 0.5 g of

TbCl₃·6H₂O was placed in an alumina crucible, heated to 400°C at 5°C min⁻¹, held for 8 h, and then cooled to room temperature at 5°C min⁻¹. This synthesis method was used in our previous study (Riley *et al.*, 2018). The resulting product was a light-brown powder, which was ground in a mortar and pestle for X-ray powder diffraction analysis.

4. Refinement

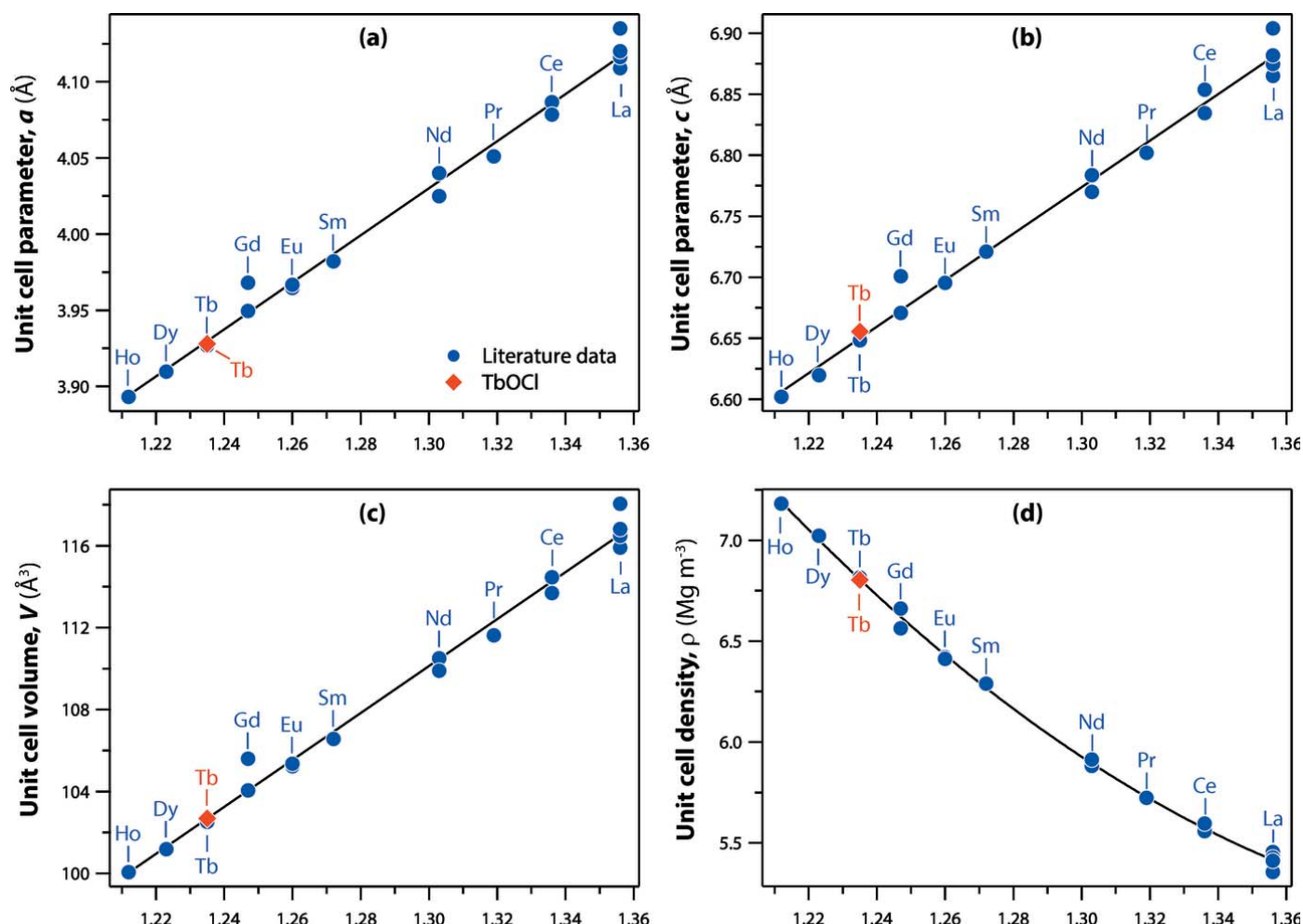
Crystal data, data collection and structure refinement details are summarized in Table 2. The unit-cell parameters were obtained using TOPAS (version 4.2; Bruker, 2009) by refining the GdOCl pattern (ICSD 77820) with geometrical and chemical resemblance as a starting model. The Rietveld refinement was performed using JANA2006 (Petříček *et al.*, 2014) with the obtained unit-cell parameters as initial values.

**Figure 2**

The RE–Cl and RE–O bond lengths in the REOCl compounds listed in Table 1 as a function of RE crystal radius (coordination = 9) according to Shannon (1976). Where multiple values were available, averages and standard deviations are included for the datapoints. For (a), 1-nd and 4-nd denote 1 and 4 neighbor distances, respectively

Table 1Structural parameters of $RE\text{OCl}$ compounds.All compounds crystallize in the $P4/nmm$ space group. For the $RE\text{--Cl}$ bond lengths, the first value refers to one neighboring Cl atom, and the second number refers to four neighboring Cl atoms. Densities are calculated from crystallographic data.

RE	a (Å)	c (Å)	V (Å 3)	Density (g cm $^{-3}$)	$RE\text{--O}$ (Å)	$RE\text{--Cl}$ (Å)	$\text{Cl}\cdots\text{Cl}$ (Å)	$\text{Cl}\cdots\text{O}$ (Å)	$\text{O}\cdots\text{O}$ (Å)	ICSD/PDF
Ho	3.893	6.602	100.1	7.182	2.247	3.04, 3.05	3.24	3.12	2.753	76171 (Templeton & Dauben, 1953)
Dy	3.91	6.62	101.2	7.023						00-047-1725 (Kirik <i>et al.</i> , 1996)
Tb	3.9269	6.648	102.5	6.815						00-048-1648 (Kirik <i>et al.</i> , 1996)
Tb	3.9279	6.6556	102.7	6.804	2.2649	3.064, 3.082	3.271	3.151	2.7774	Current study
Gd	3.9495	6.6708	104.1	6.661	2.2839	3.036, 3.098	3.267	3.176	2.7927	59232 (Meyer & Schleid, 1986)
Gd	3.9698	6.7008	105.6	6.564	2.28	3.212, 3.071	3.428	3.089	2.8071	77820 (Hölsä <i>et al.</i> , 1996)
Eu	3.9646	6.695	105.2	6.42	2.286	3.08, 3.11	3.3	3.17	2.8034	28529 (Bärnighausen <i>et al.</i> , 1965)
Eu	3.9668	6.6955	105.4	6.412	2.2901	3.062, 3.1103	3.289	3.183	2.80492	54682 (Schnick, 2004)
Sm	3.982	6.721	106.6	6.289	2.296	3.09, 3.12	3.31	3.19	2.8157	26581 (Templeton & Dauben, 1953)
Nd	4.04	6.77	110.5	5.882	2.359	3.114, 3.11	3.428	3.165	2.86	31665 (Zachariasen, 1949)
Nd	4.0249	6.7837	109.9	5.914	2.3362	3.082, 3.141	3.343	3.221	2.84603	59231 (Meyer & Schleid, 1986)
Pr	4.053	6.799	111.7	5.723	2.3674	3.128, 3.116	3.441	3.178	2.866	31664 (Zachariasen, 1949)
Ce	4.0866	6.8538	114.5	5.558	2.3687	3.1190, 3.1846	3.3942	3.2572	2.8897	412069 (Schnick, 2004)
Ce	4.0785	6.8346	113.7	5.596	2.36413	3.103, 3.180	3.38	3.254	2.88393	72154 (Wolcyrz & Kepinski, 1992)
La	4.109	6.865	115.9	5.454	2.39	3.14, 3.18	3.45	3.24	2.9055	24611 (Sillen & Nylander, 1941)
La	4.117	6.881	116.6	5.42	2.3866	3.126, 3.2046	3.416	3.2751	2.9112	40297 (Brixner & Moore, 1983)
La	4.1351	6.904	118.1	5.355	2.395	3.165, 3.209	3.457	3.268	2.92397	77815 (Hölsä <i>et al.</i> , 1996)
La	4.1162	6.8746	116.5	5.428	2.3832	3.138, 3.201	3.425	3.265	2.9106	84330 (Hölsä <i>et al.</i> , 1997)
La	4.12	6.882	116.8	5.412						00-008-0477 (Swanson <i>et al.</i> , 1957)

**Figure 3**(a, b) Unit-cell parameters (a and c , respectively), (c) unit-cell volumes, and calculated unit-cell densities as a function of the crystal radius of the RE (coordination = 9) according to Shannon (1976) compared to literature values provided in Table 1.

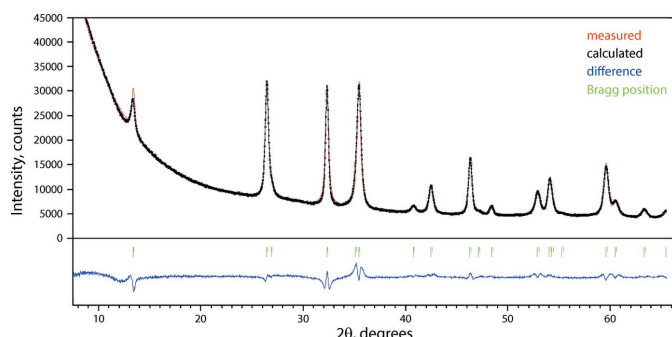


Figure 4
Measured, calculated, and difference XRD patterns of TbOCl.

A pseudo-Voigt function with other peak-shape parameters were used to fit peaks, and the background was modeled with a Chebychev polynomial. The plot of the Rietveld refinement result is shown in Fig. 4. The final refinement converged at $R_{wp} = 3.22\%$.

Acknowledgements

The Pacific Northwest National Laboratory is operated by Battelle under Contract Number DE-AC05-76RL01830.

References

- Au, C. T., He, H., Lai, S. Y. & Ng, C. F. (1997). *Appl. Catal. Gen.* **159**, 133–145.
- Bannister, F. A. (1934). *Miner. Mag. j. Miner. Soc.* **23**, 587–597.
- Bärnighausen, H., Brauer, G. & Schultz, N. (1965). *Z. Anorg. Allg. Chem.* **338**, 250–265.
- Berdowski, P. A. M., van Herk, J., Jansen, L. & Blasse, G. (1984). *Phys. Status Solidi B*, **125**, 387–391.
- Brixner, L. H. & Moore, E. P. (1983). *Acta Cryst. C* **39**, 1316.
- Bruker (2009). TOPAS. Bruker AXS, Karlsruhe, Germany.
- Hölsä, J., Lastusaari, M. & Valkonen, J. (1997). *J. Alloys Compd.* **262**, 299–304.
- Hölsä, J., Säilynoja, E., Koski, K., Rahiala, H. & Valkonen, J. (1996). *Powder Diffr.* **11**, 129–133.
- Imanaka, N., Okamoto, K. & Adachi, G. (2001a). *Chem. Lett.* **30**, 130–131.
- Imanaka, N., Okamoto, K. & Adachi, G. (2001b). *Electrochim. Commun.* **3**, 49–51.
- Kienle, M. & Jacob, M. (2003). *XRD Commander*. Bruker AXS GmbH, Karlsruhe, Germany.
- Kim, D., Jeong, J. R., Jang, Y., Bae, J.-S., Chung, I., Liang, R., Seo, D.-K., Kim, S.-J. & Park, J.-C. (2019). *Phys. Chem. Chem. Phys.* **21**, 1737–1749.
- Kim, D., Park, S., Kim, S., Kang, S.-G. & Park, J.-C. (2014). *Inorg. Chem.* **53**, 11966–11973.
- Kirik, S., Yakimov, I., Blochin, A. & Soloyov, L. (1996). ICDD Grant-in-Aid, Institute of Chemistry, Krasnoyarsk, Russia.
- Marsal, A., Centeno, M. A., Odriozola, J. A., Cornet, A. & Morante, J. R. (2005). *Sens. Actuators B Chem.* **108**, 484–489.
- Maslen, E. N., Streltsov, V. A., Streltsova, N. R. & Ishizawa, N. (1996). *Acta Cryst. B* **52**, 576–579.
- Meyer, G. & Schleid, T. (1986). *Z. Anorg. Allg. Chem.* **533**, 181–185.
- Momma, K. & Izumi, F. (2011). *J. Appl. Cryst.* **44**, 1272–1276.
- Okamoto, K., Imanaka, N. & Adachi, G. (2002). *Solid State Ionics*, **154–155**, 577–580.
- Palatinus, L. & Chapuis, G. (2007). *J. Appl. Cryst.* **40**, 786–790.
- Peringer, E., Salzinger, M., Hutt, M., Lemonidou, A. A. & Lercher, J. A. (2009). *Top. Catal.* **52**, 1220–1231.
- Petříček, V., Dusek, M. & Palatinus, L. (2014). *Z. Kristallogr.* **229**, 345–352.
- Podkolzin, S. G., Stangland, E. E., Jones, M. E., Peringer, E. & Lercher, J. A. (2007). *J. Am. Chem. Soc.* **129**, 2569–2576.
- Riley, B. J., Pierce, D. A., Crum, J. V., Williams, B. D., Snyder, M. M. V. & Peterson, J. A. (2018). *Prog. Nucl. Energy*, **104**, 102–108.
- Scharfe, M., Lira-Parada, P. A., Amrute, A. P., Mitchell, S. & Pérez-Ramírez, J. (2016). *J. Catal.* **344**, 524–534.
- Schnick, W. (2004). Private Communication.
- Shannon, R. D. (1976). *Acta Cryst. A* **32**, 751–767.
- Sillen, L. G. & Nylander, A. L. (1941). *Svensk Kemisk Tidskrift*, **53**, 367–372.
- Swanson, H. E., Gilfrich, N. T. & Cook, M. I. (1957). *Circ. Bur. Stand.* pp. 539.
- Templeton, D. H. & Dauben, C. H. (1953). *J. Am. Chem. Soc.* **75**, 6069–6070.
- Westrip, S. P. (2010). *J. Appl. Cryst.* **43**, 920–925.
- Wołczyk, M. & Kepinski, L. (1992). *J. Solid State Chem.* **99**, 409–413.
- Zachariasen, W. H. (1949). *Acta Cryst.* **2**, 388–390.

Table 2
Experimental details.

Crystal data	TbOCl
Chemical formula	$M_r = 210.4$
Crystal system, space group	Tetragonal, $P4/nmm$
Temperature (K)	293
a, c (Å)	3.9279 (2), 6.6556 (5)
V (Å 3)	102.68 (1)
Z	2
Radiation type	$\text{Cu } K\alpha, \lambda = 1.54188$ Å
Specimen shape, size (mm)	Cylinder, 25 × 25
Data collection	Bruker D8 Advance
Diffractometer	Packed powder pellet
Specimen mounting	Reflection
Data collection mode	Step
Scan method	2θ values (°)
	$2\theta_{\min} = 5, 2\theta_{\max} = 68.977,$ $2\theta_{\text{step}} = 0.019$
Refinement	
R factors and goodness of fit	$R_p = 0.020, R_{wp} = 0.032,$ $R_{\text{exp}} = 0.009, R(F) = 0.033,$ $\chi^2 = 13.690$
No. of parameters	17

Computer programs: *XRD Commander* (Kienle & Jacob, 2003), *TOPAS* (Bruker, 2009), *SUPERFLIP* (Palatinus & Chapuis, 2007), *JANA2006* (Petříček *et al.*, 2014), *VESTA* (Momma & Izumi, 2011) and *publCIF* (Westrip, 2010).

supporting information

Acta Cryst. (2020). E76, 621-624 [https://doi.org/10.1107/S2056989020004387]

Dehydration synthesis and crystal structure of terbium oxychloride, TbOCl

Saehma Chong, Brian J. Riley and Zayne J. Nelson

Computing details

Data collection: *XRD Commander* (Kienle & Jacob, 2003); cell refinement: *TOPAS* (Bruker, 2009); program(s) used to solve structure: SUPERFLIP (Palatinus & Chapuis, 2007); program(s) used to refine structure: JANA2006 (Petříček *et al.*, 2014); molecular graphics: *VESTA* (Momma & Izumi, 2011); software used to prepare material for publication: *publCIF* (Westrip, 2010).

Terbium oxychloride

Crystal data

TbOCl	Z = 2
$M_r = 210.4$	$D_x = 6.804 \text{ Mg m}^{-3}$
Tetragonal, $P4/nmm$	Cu $K\alpha$ radiation, $\lambda = 1.54188 \text{ \AA}$
$a = 3.9279 (2) \text{ \AA}$	$T = 293 \text{ K}$
$c = 6.6556 (5) \text{ \AA}$	light brown
$V = 102.68 (1) \text{ \AA}^3$	cylinder, $25 \times 25 \text{ mm}$

Data collection

Bruker D8 Advance	Data collection mode: reflection
diffractometer	Scan method: step
Radiation source: sealed X-ray tube	$2\theta_{\min} = 5^\circ$, $2\theta_{\max} = 68.977^\circ$, $2\theta_{\text{step}} = 0.019^\circ$
Specimen mounting: packed powder pellet	

Refinement

$R_p = 0.020$	17 parameters
$R_{wp} = 0.032$	Weighting scheme based on measured s.u.'s
$R_{\text{exp}} = 0.009$	$(\Delta/\sigma)_{\max} = 0.030$
$R(F) = 0.033$	Background function: 8 Chebyshev polynomials
3292 data points	Preferred orientation correction: March &
Profile function: Pseudo-Voigt	Dollase

Fractional atomic coordinates and isotropic or equivalent isotropic displacement parameters (\AA^2)

	x	y	z	$U_{\text{iso}}^*/U_{\text{eq}}$
Tb1	0.5	0	0.3305 (2)	0.002
Cl1	0	0.5	0.1298 (9)	0.002
O1	1	0	0.5	0.002

Atomic displacement parameters (\AA^2)

	U^{11}	U^{22}	U^{33}	U^{12}	U^{13}	U^{23}
Tb1	0.002	0.002	0.002	0	0	0
Cl1	0.002	0.002	0.002	0	0	0
O1	0.002	0.002	0.002	0	0	0

Geometric parameters (\AA , $^\circ$)

Tb1—Tb1 ⁱ	3.5784 (13)	Tb1—O1 ^v	2.2649 (7)
Tb1—Tb1 ⁱⁱ	3.5784 (13)	Tb1—O1	2.2649 (7)
Tb1—Tb1 ⁱⁱⁱ	3.5784 (13)	Tb1—O1 ^{vi}	2.2649 (7)
Tb1—Tb1 ^{iv}	3.5784 (13)	Tb1—O1 ^{vii}	2.2649 (7)
Tb1 ⁱ —Tb1—Tb1 ⁱⁱ	66.57 (2)	Tb1 ⁱⁱⁱ —Tb1—O1 ^{vii}	99.31 (4)
Tb1 ⁱ —Tb1—Tb1 ⁱⁱⁱ	66.57 (2)	Tb1 ^{iv} —Tb1—O1 ^v	99.31 (4)
Tb1 ⁱ —Tb1—Tb1 ^{iv}	101.82 (4)	Tb1 ^{iv} —Tb1—O1	37.817 (14)
Tb1 ⁱ —Tb1—O1 ^v	37.817 (14)	Tb1 ^{iv} —Tb1—O1 ^{vi}	99.31 (4)
Tb1 ⁱ —Tb1—O1	99.31 (4)	Tb1 ^{iv} —Tb1—O1 ^{vii}	37.817 (14)
Tb1 ⁱ —Tb1—O1 ^{vi}	37.817 (14)	O1 ^v —Tb1—O1	120.25 (6)
Tb1 ⁱ —Tb1—O1 ^{vii}	99.31 (4)	O1 ^v —Tb1—O1 ^{vi}	75.63 (3)
Tb1 ⁱⁱ —Tb1—Tb1 ⁱⁱⁱ	101.82 (4)	O1 ^v —Tb1—O1 ^{vii}	75.63 (3)
Tb1 ⁱⁱ —Tb1—Tb1 ^{iv}	66.57 (2)	O1—Tb1—O1 ^{vi}	75.63 (3)
Tb1 ⁱⁱ —Tb1—O1 ^v	37.817 (14)	O1—Tb1—O1 ^{vii}	75.63 (3)
Tb1 ⁱⁱ —Tb1—O1	99.31 (4)	O1 ^{vi} —Tb1—O1 ^{vii}	120.25 (6)
Tb1 ⁱⁱ —Tb1—O1 ^{vi}	99.31 (4)	Tb1—O1—Tb1 ^{viii}	120.25 (4)
Tb1 ⁱⁱ —Tb1—O1 ^{vii}	37.817 (14)	Tb1—O1—Tb1 ⁱⁱⁱ	104.37 (2)
Tb1 ⁱⁱⁱ —Tb1—Tb1 ^{iv}	66.57 (2)	Tb1—O1—Tb1 ^{iv}	104.37 (2)
Tb1 ⁱⁱⁱ —Tb1—O1 ^v	99.31 (4)	Tb1 ^{viii} —O1—Tb1 ⁱⁱⁱ	104.37 (2)
Tb1 ⁱⁱⁱ —Tb1—O1	37.817 (14)	Tb1 ^{viii} —O1—Tb1 ^{iv}	104.37 (2)
Tb1 ⁱⁱⁱ —Tb1—O1 ^{vi}	37.817 (14)	Tb1 ⁱⁱⁱ —O1—Tb1 ^{iv}	120.25 (4)

Symmetry codes: (i) $-x+1/2, y-1/2, -z+1$; (ii) $-x+1/2, y+1/2, -z+1$; (iii) $-x+3/2, y-1/2, -z+1$; (iv) $-x+3/2, y+1/2, -z+1$; (v) $x-1, y, z$; (vi) $-y+1/2, x-3/2, z$; (vii) $-y+1/2, x-1/2, z$; (viii) $x+1, y, z$.